Palladium(II) Complexes with the 4,5-Bis(diphenylphosphino)acenaphthene Ligand and Their Reactivity with Ethylene

Anna Dall'Anese,[a] Massimo Tosolini,[a] Chiara Alberoni,[a] Gabriele Balducci,[a] Maurizio Polentarutti,[b] Claudio Pellecchia,[c, d] Paolo Tecilla,[a] and Barbara Milani*[a, d]

The last two decades have witnessed the development of homogeneous catalysts for ethylene homo- and co-polymerization reactions based on late transition metals. When Pd(II) is the metal of choice, the best ligand-metal combination deals with either bidentate nitrogen-donor molecules or phosphinobenzene sulfonate derivatives. In this contribution we have investigated the coordination chemistry to Pd(II) of a bidentate phosphorus ligand, namely 4,5-bis(diphenylphosphino)acenaphthene (**1**). Starting from the neutral complex, [Pd(**1**)(CH_3)Cl], we obtained the cationic derivatives [Pd(**1**)(CH_3)(L)][SbF_6], with L being either CH_3CN or 3,5-lutidine. Using *in situ* NMR spectroscopy we investigated the reaction of [Pd(**1**)(CH_3)($NCCH_3$)][SbF_6] with ethylene, at room temperature, and ambient ethylene pressure. We discovered that [Pd(**1**)(CH_3)($NCCH_3$)][SbF_6] acts as a catalyst for butenes and hexenes synthesis with the relevant Pd-ethyl intermediate as the catalyst resting state. At the same time the color of the solution turned from pale yellow to light red due to the formation of the dinuclear species [Pd(μ-η^2–C_6H_5)PPh)–PPh_2]$_2$[SbF_6]$_2$. Both the neutral Pd(II) complex, activated in situ by $NaSbF_6$, and the monocationic acetonitrile derivative were tested in the ethylene homopolymerization reaction at high pressure, leading to low molecular weight, branched, polyethylene.

Introduction

The last two decades have witnessed a huge development of Pd(II) complexes applied as homogeneous catalysts for ethylene homo- and co-polymerization reactions, and a relationship between the monomer nature and the ancillary ligand present in the metal ion coordination sphere could be established. Indeed, when ethylene homopolymerization is the target reaction, the best performing Pd-catalysts are based on bidentate ligands belonging to the family of either α-diimines (N–N, **L1**–**L4**, Figure 1)[1] or phosphinobenzene sulfonate (P–O, **L5**, Figure 1)[2] derivatives leading to branched or linear polyethylene, respectively. The same families of ligands can impart superior catalytic properties to palladium making it able to catalyze the direct, controlled copolymerization of ethylene with a variety of polar vinyl monomers leading to functionalized polyolefins.[3] More recently, other classes of ligands were also considered, e.g. bisphosphine monoxide (**L6**, Figure 1),[4] phosphine-phosphonic amide and diamide (**L7** and **L8**, Figure 1),[5] and a few examples of chelating NHC carbenes (**L9** and **L10**, Figure 1).[6]

On the other hand, in the copolymerization of ethylene with carbon monoxide to yield perfectly alternating polyketones, the best performing catalysts (leading to the industrial exploitation of the reaction) are based on palladium(II) complexes with bidentate phosphorus-donor ligand (P–P), e.g. 1,3-bis(diphenyl)phosphino propane (**L11**, Figure 1) or its anisole-substituted derivative.[7]

As for the use of phosphines as ancillary ligands of catalysts based on late transition metals for ethylene oligomerization and homopolymerization, some remarkable examples of Ni(II) complexes have been reported. In addition to the bulky phosphino-based SHOP catalysts[8] and the bulky iminophosphine-Ni complexes,[9] they also include catalysts based on either bidentate[10] or monodentate phosphines.[11] On the other hand, to the best of our knowledge only a few examples of the use of Pd(II) can be found. They involve both hybrid P–X and bidentate P–P ligands. Examples of ligands of the P–X family are phosphine-iminophosphoranes (P–N, **L12**, Figure 1),[12] phosphine-sulfonamide derivatives (**L13**–**L15**, Figure 1)[13] and modified P–O molecules. The latter class includes both a P–O derivative bearing one aryl ring substituted with a diethyl phosphonate group which has an additional donor atom (**L16**, Figure 1),[14] and a P–O molecule where one of the sulfonate oxygen atoms is linked to the boron atom of the Lewis acid [$B(C_6F_5)_3$] (**L17**, Figure 1).[15] For the latter, the introduction of the

[a] *Dr. A. Dall'Anese, Dr. M. Tosolini, C. Alberoni, Dr. G. Balducci, Prof. Dr. P. Tecilla, Prof. Dr. B. Milani*
Department of Chemical and Pharmaceutical Sciences, University of Trieste
Via Licio Giorgieri 1, 34127 Trieste, Italy
E-mail: milaniba@units.it
[b] *Dr. M. Polentarutti*
Elettra, Sincrotrone Trieste
S.S. 114 km 163.5, Basovizza, 34149 Trieste, Italy
[c] *Prof. Dr. C. Pellecchia*
Department of Chemistry and Biology "Adolfo Zambelli",
University of Salerno
Via Giovanni Paolo II 132, 84084 Fisciano (SA), Italy
[d] *Prof. Dr. C. Pellecchia, Prof. Dr. B. Milani*
Consorzio per la Reattività Chimica e la Catalisi CIRCC
Via Celso Ulpiani 27, 70126 Bari, Italy

Supporting information for this article is available on the WWW under https://doi.org/10.1002/ejic.202200481

Part of the Institute Feature highlighting the "Interuniversity Consortium in Chemical Reactivity and Catalysis (CIRCC)".

Lewis acid resulted in the shift of the catalytic behavior of the complex from being a catalyst for ethylene polymerization to a more active catalyst for oligomerization. Finally, the use of an atropoisomeric, bulky diphosphine (**L18**, Figure 1) allowed to obtain hyperbranched ethylene oligomers with an M_n of ca. 300 Da, and the catalyst proved to be resistant up to 348 K.[16]

Very recently some of us have studied the coordination chemistry of 4,5-bis(diphenylphosphino)acenaphthene, **1** (Figure 1), to [Ni(cod)Cl_2], [Pd(cod)Cl_2], [Pt(cod)Cl_2] and [CuCl] together with the photophysical properties and ionophoric activity of the obtained complexes. Ligand **1** was shown to form square planar complexes with group 10 metal ions ([M(**1**)Cl_2] with M=Ni(II), Pd(II), Pt(II)) and a dimeric tetrahedral complex with Cu(I). In all the complexes the rigid acenaphthene backbone forces the two phosphorus atoms at a distance well below twice their van der Waals radius. Among the complexes, [Cu(**1**)Cl]$_2$ is the only one that displays weak fluorescence in solution and high photoluminescence quantum yield in the solid state due to the contribution of thermally-activated delayed fluorescence. Moreover, [Pd(**1**)Cl_2] and [Cu(**1**)Cl]$_2$ behave as chloride transporters across a phospholipid membrane with the Pd(II) complex displaying a higher activity.[17]

1 is a sterically encumbered molecule having an acenaphthene skeleton, which is one of the typical motives found in the class of the α-diimine molecules applied as ancillary ligands for palladium catalysts for both ethylene homopolymerization and ethylene/acrylic esters copolymerization to yield functionalized polyolefins.[3c,18] In particular, the X-ray analysis of [Pd(**1**)Cl_2], reported in the previous investigation,[17] showed that upon coordination of ligand **1** to the Pd ion, two phenyl rings, one per each P atom, assume an orientation which is orthogonal to the square plane of the Pd atom and mutually parallel, stabilized by a π-π stacking interaction (Figure 2c). In addition, the acenaphthene moiety bends with respect to the Pd square plane (dihedral angle: 37.5°). This represents a remarkable difference with respect to the α-diimine ligands (BIAN, **L2**, Figure 1 and Figure 2a), where the acenaphthene skeleton is coplanar with the palladium coordination plane.[19] In a similar way, although the geometry of the distortion is different, a significant loss of coplanarity between the coordination environment of the metal atom and the organic ligand skeleton is observed for the Pd complexes with the phenanthrene-derived α-diimines (BIP, **L3**, Figure 1 and Figure 2b); a positive effect of the distortion on the catalytic behavior has been conjectured in this latter case.[20]

Therefore, we have now used **1** to synthesize both neutral and monocationic organometallic palladium(II) complexes to be tested in both ethylene homopolymerization and in their *in situ* NMR reactivity with this alkene to gain some mechanistic information.

Barbara Milani is Associate Professor of General and Inorganic Chemistry at the University of Trieste. She received her PhD degree at University of Trieste in 1994. After a post-doctoral period, she became assistant professor in 1998 and in 2014 she was promoted associate professor. She was visiting professor at Institut National Polytechnique in Toulouse in 2010 and at Universitè Pierre et Marie Curie in Paris in 2014. In 2017 she got the National Habilitation to Full Professor of General and Inorganic Chemistry. She was member of the Advisory Board of European Journal of Inorganic Chemistry (2007–2009). Currently, she is member of the Advisory Board of Dalton Transactions. She was the coordinator of the PhD School Doctorate in Chemistry (joint PhD School between University of Trieste and Ca' Foscari University Venice; 2017–2019). She is the ERASMUS coordinator for chemistry for the Department of Chemical and Pharmaceutical Sciences @UniTS. Her main research interests focus on organometallic chemistry and on development of homogeneous catalysts, based on late transition metals, for polymerization reactions.

Results and Discussion

Synthesis and Characterization of Pd(II) complexes with ligand 1

Ligand **1** was synthesized according to the reported literature procedure,[17] and used to obtain complex **1a**, [Pd(**1**)(CH_3)Cl], following the synthetic methodology usually employed to prepare the analogous Pd(II) complexes with α-diimine ligands.[21] The complex was characterized by mono- and bidimensional NMR spectroscopy (Scheme 1).

In the ^{1}H-NMR spectrum of the solid isolated from the synthesis only one set of signals is present (Figure S3), and the resonance of Pd–CH_3 is easily recognized based on both its chemical shift (0.51 ppm) and multiplicity (a doublet of doublets, J = 8.1, 3.4 Hz) originated by the coupling with the two inequivalent phosphorus atoms. At 3.46 ppm a broad peak due to the methylene protons of the ligand backbone is present, and it resonates at a frequency slightly higher than that of the same signal in the free ligand (3.40 ppm); a similar change is also found for the resonances of the aromatic protons of both the acenaphthene skeleton and the phenyl rings. The P atoms of the ligand generate two doublets in the ^{31}P-NMR spectrum (29.0 and 1.4 ppm, J_{PP} = 65 Hz; Figure S4).

Starting from **1a** the cationic complex **1b**, [Pd(**1**)(CH_3)($NCCH_3$)][SbF_6], was obtained through a dehalogenation reaction, in the presence of $AgSbF_6$ and acetonitrile. Differently from the neutral precursor, in this case the ^{1}H-NMR spectrum displays two sets of signals (Figure S6): other than the expected peaks of the cationic complex (the singlet of Pd–CH_3 at 0.51 ppm, and the broad signals at 1.84 and 3.52 ppm for Pd-$NCCH_3$ and the methylene protons of bonded **1**, respectively), a rather broad signal at −1.98 ppm together with the resonance of methane (0.21 ppm) suggest the formation of another organometallic compound. This is further confirmed by the ^{31}P-NMR spectrum (Figure S7), where the two doublets for **1b** are present (at 29.8 and −0.1 ppm), along with a singlet at

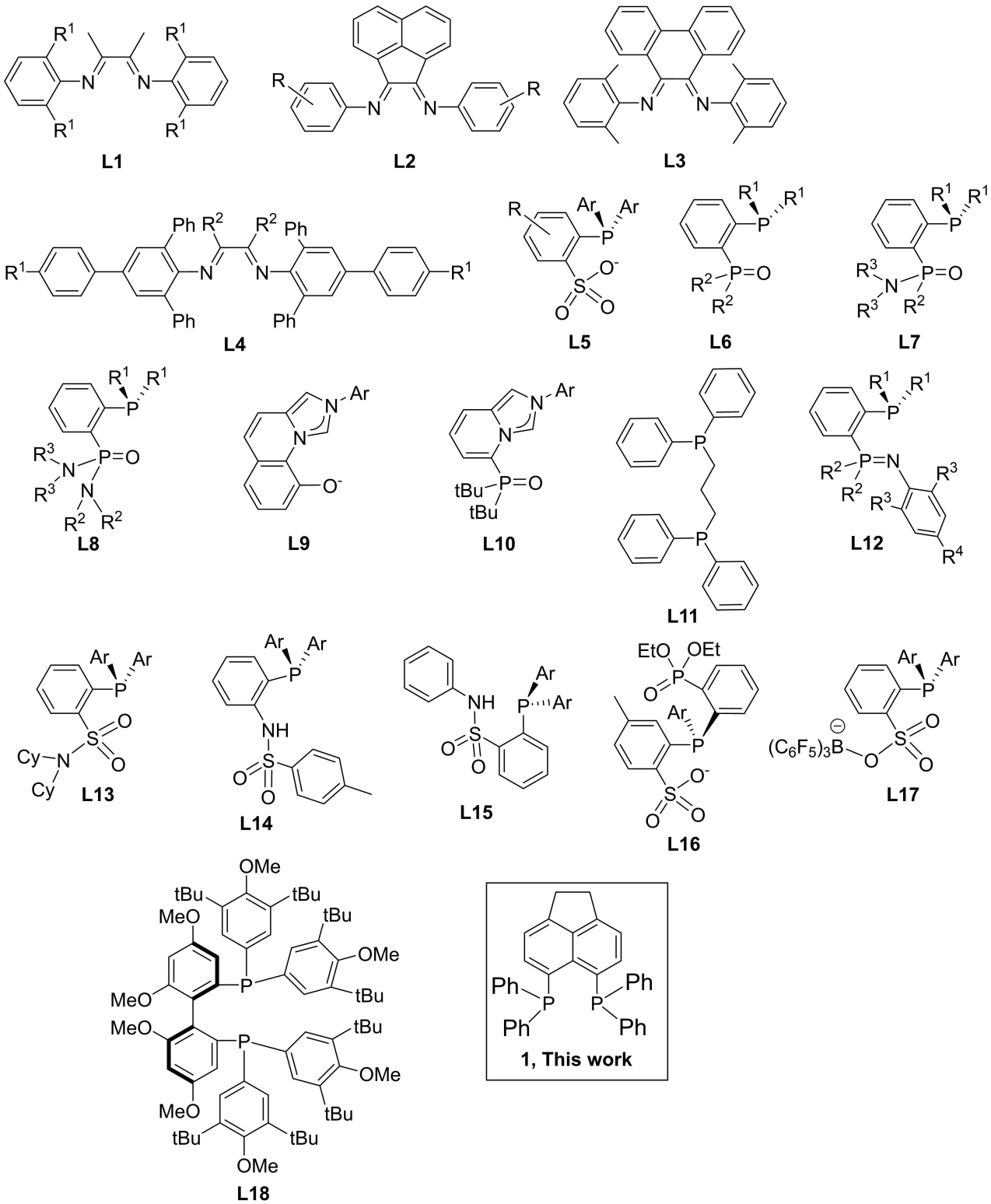

Figure 1. Some examples of ancillary ligands for Pd(II) catalysts for homo- and copolymerization reactions.

20.1 ppm, suggesting the high symmetry of the second species formed. These findings allowed us to consider the formation of species **2**, namely $[Pd(\mathbf{1})(\mu\text{-}OH)]_2[SbF_6]_2$, since it is known from literature[22] that Pd(II) organometallic complexes bearing diphosphine ligands of the series $[Pd(P'–P')(CH_3)(NCCH_3)][PF_6]$ (P′–P′ = 1,3-bis(diphenylphosphino)propane, *meso*-1,3-bis(diphenylphosphino)pentane, *rac*-1,3-bis(diphenylphosphino)pentane) in presence of water can

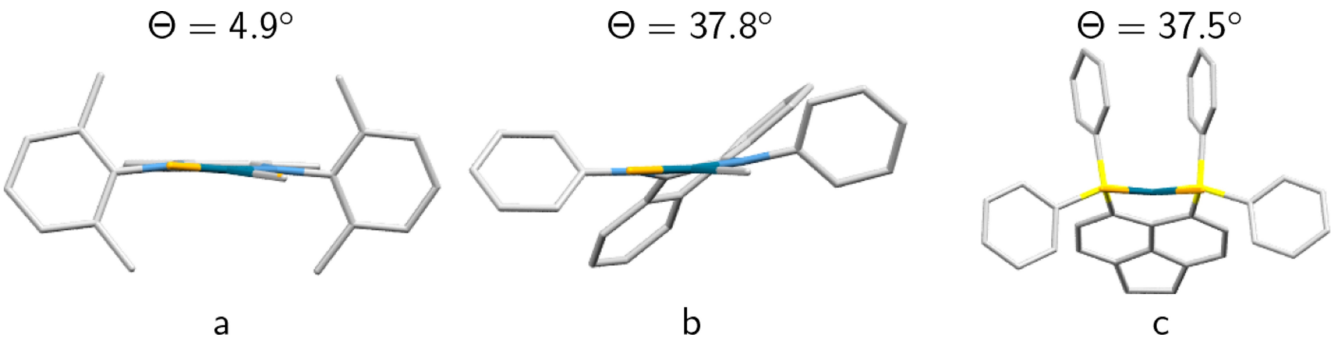

Figure 2. Comparison of the molecules of complexes [Pd(**L2**)(CH_3)Cl] (a), [Pd(**L3**)(CH_3)Cl] (b) and [Pd(**1**)Cl_2] (c) in the solid state. Θ values are for the dihedral angle between the average planes through the Pd with its four bonded atoms and the ancillary ligand.

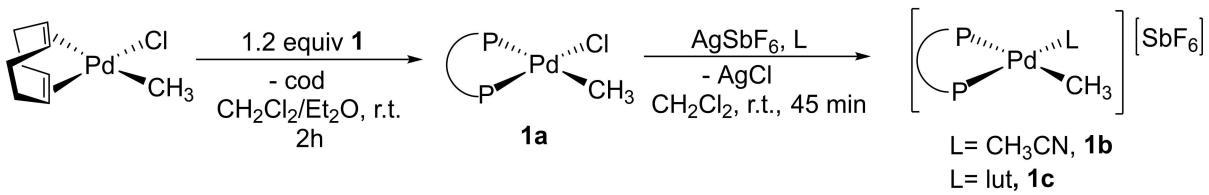

Scheme 1. Synthesis of the neutral and cationic Pd(II) complexes with ligand **1**.

convert to dinuclear species having hydroxo bridges, namely [Pd(P′–P′)(μ-OH)]$_2$[PF_6]$_2$. After 25 h in solution at room temperature, **1 b** completely converts to species **2** (Figure S9, Figure S10).

To have a better understanding of this process, a kinetic study using *in situ* NMR spectroscopy was performed. A 10 mM solution of **1 b** was prepared using commercial CD_2Cl_2 containing 100 ppm H_2O and the conversion was monitored by ^{1}H-NMR spectroscopy for two hours. In agreement with our previous observation, **1 b** converts to **2** over this time, with an observed kinetic constant of $k_{obs} = 0.0554\ s^{-1}$ (Figure 3 and Figure S12).

The formation of the dimeric species **2** was also confirmed by: (i) the 1D-NOESY spectrum (Figure S15) recorded upon irradiation of the signal at −1.98 ppm, and resulting in an Overhauser effect between the Pd–OH fragment and the protons of the phenyl substituents on the P atoms (7.16 ppm); (ii) an exchange experiment performed upon addition of an excess of D_2O (Figure S16), resulting in the disappearance of the signal at −1.98 ppm, in agreement with the H–D exchange; (iii) a ^{1}H,^{1}H-NOESY experiment where an exchange peak between the signals of μ-OH and H_2O, present in traces in CD_2Cl_2, is observed (Figure S17).

Moreover, upon stratification of n-hexane over the CD_2Cl_2 solution of **2**, after two weeks at 277 K, single crystals suitable for X-ray analysis were obtained.

The molecular structure of **2** in the solid state (Figure 4) agrees with the one observed in solution and confirms the formation of a dinuclear species where the hydroxo-bridged Pd(II) ions have the expected square planar geometry, with bond angles close to 90°. Comparing the structure to that reported for [Pd(**1**)Cl_2],[17] Pd–P distances in **2** are shorter with respect to those in the dichloride complex (Pd1–P11 2.2115(6), Pd1–P12 2.2115(6), Pd2–P21 2.2212(6), Pd2–P22 2.2236(6) Å for **2**, Pd–P1 2.2384(4), Pd–P2 2.2430(5) Å for [Pd(**1**)Cl_2]), in agreement with the change in the charge of the complex. Similarly to what was previously reported, also for complex **2** the acenaphthene backbone is not coplanar with the coordination planes of the two palladium ions, forming angles of 29.99(6)° and 48.24(5)° for Pd1 and Pd2, respectively.

The distance between the two Pd ions (3.1685(3) Å) is short enough to indicate the presence of metal-metal interactions.[23] On each mononuclear fragment two phenyl substituents, one per each P atom, face parallel to each other and orthogonal to the Pd coordination plane; the centroid-centroid distances (3.640 Å for Ph(12)–Ph(14) and 3.507 Å for Ph(22)–Ph(24)) indicate the presence of π-π stacking.[24] The bending of both **1** ligands with respect to the corresponding Pd coordination plane (dihedral angles quoted in the caption of Figure 4) makes them assume an "*anti*" conformation with respect to the average plane defined by the Pd ions and the hydroxo bridges. A similar coordination of **1** was observed in the dimeric species [Cu(**1**)Cl]$_2$.[17] Finally, the analysis of crystal packing points out that the hydrogen atom in para position of one of the phenyl substituents in one molecule is at the distance of 3.074 Å from the centroid of the phenyl in nearest neighbor molecule suggesting a possible T-shape interaction (Figure S30).[24]

To avoid the formation of **2**, the dehalogenation reaction of **1 a** was performed in presence of 3,5-lutidine (lut) instead of acetonitrile, leading to the isolation of [Pd(**1**)(CH_3)(lut)][SbF_6], **1 c**. In the ^{1}H-NMR spectrum of the CD_2Cl_2 solution of the yellow solid isolated from the synthetic mixture, the signals of only one species are observed (Figures S18, S19). In the aliphatic region the resonances of Pd–CH_3 (dd at 0.48 ppm), methyl

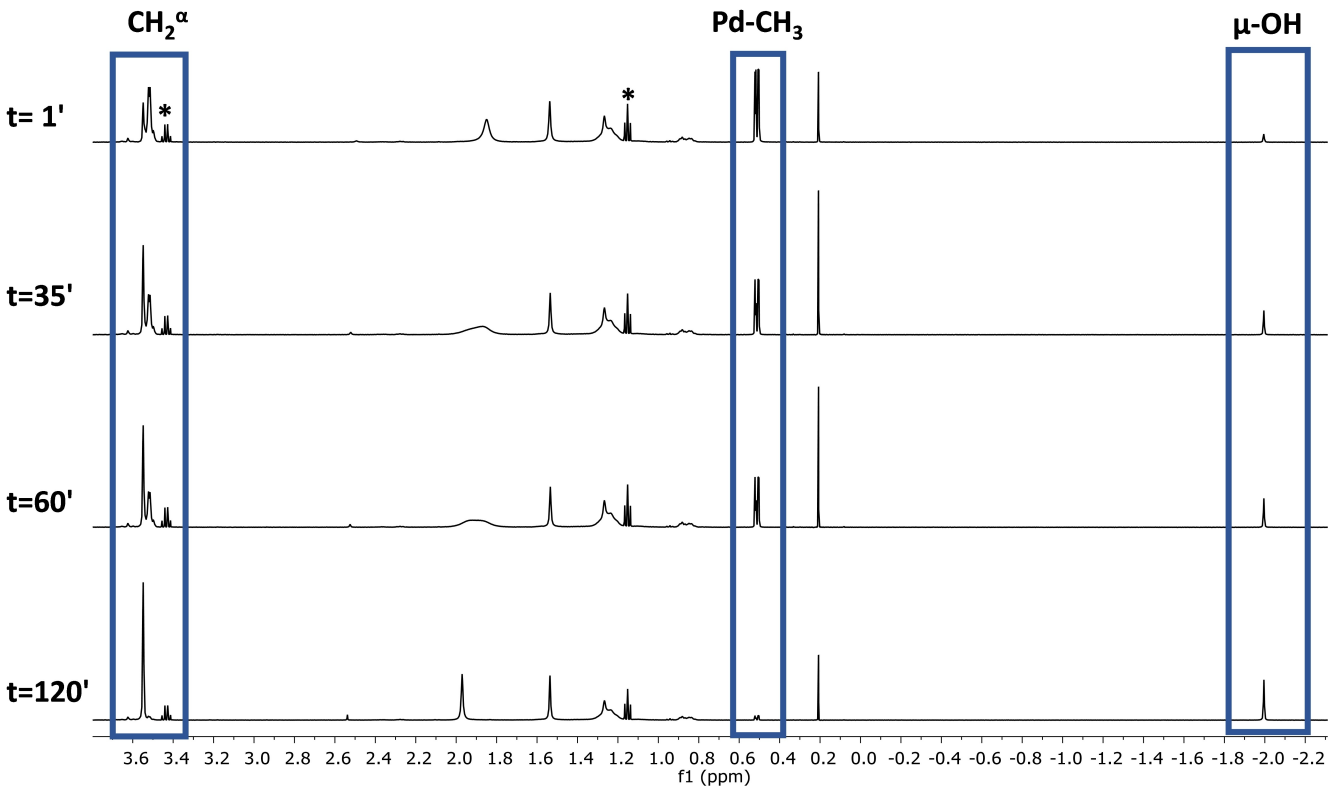

Figure 3. ^{1}H-NMR spectra in CD_2Cl_2, 10 mM, 298 K, of [Pd(**1**)(CH_3)($NCCH_3$)][SbF_6] **1 b**: conversion to **2** over time (* = diethyl ether).

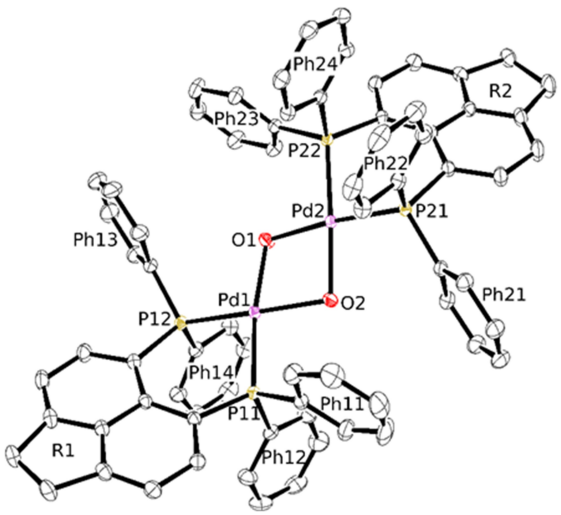

Figure 4. ORTEP representation (50 % probability ellipsoids) of the molecule of complex **2** in the crystal structure. Selected bond distances (Å) and angles (°): Pd1–O1 2.076(2), Pd1–O2 2.081(2), Pd1–P11 2.2115(6), Pd1–P12 2.2115(6), Pd2–O1 2.082(2), Pd2–O2 2.082(2), Pd2–P21 2.2212(6), Pd2–P22 2.2236(6), Pd1–Pd2 3.1685(3); O1–Pd1–O2 76.93(7)°, O2–Pd1–P11 95.71(6), O1–Pd1–P12 97.49(6)°, P11–Pd1–P12 89.00(2)°, O1–Pd2–O2 76.91(8)°, O1–Pd2–P21 97.72(6), O2–Pd2–P22 97.30(6)°, P21–Pd2–P22 87.84(2)°, dihedral angles [R1]–[Pd1] 29.99(6)°, [R2]–[Pd2] 48.24(5)°.

groups in position 3 and 5 of lutidine (s at 2.10 ppm), and methylene protons of the acenaphthene backbone (br at 3.52 ppm) are present. The aromatic protons of lutidine at 7.89 ($H^{2,6}$) and 7.43 ppm (H^4) were assigned based on the long-range coupling with the relevant methyl groups (Figure S20), whereas the multiplets at lower frequencies (6.95 and 7.07 ppm) were assigned to the ortho and meta protons of two phenyl substituents on the same P atom. The correlation in ^{1}H,^{1}H-COSY (Figure S20) between the CH_2 signal at 3.52 ppm and the multiplets at 7.43 and 7.36 ppm allows to assign the latter to H^{β} protons of the acenaphthene backbone. In the ^{31}P-NMR spectrum two doublets at 28.8 and 1.84 ppm are present (Figure S22). The ^{1}H-NMR spectrum recorded after 24 h from dissolution of **1 c** does not show signals relevant to species **2**, in agreement with the expected higher inertness of **1 c** with respect to **1 b**. This observation allows us to propose that the mechanism for the conversion of **1 b** to **2** involves the substitution of acetonitrile with water, followed by protonation of Pd–CH_3 by the coordinated water molecule, with formation of methane, which leaves the coordination sphere, now completed by the hydroxo bridges (Scheme 2).

It might be noticed that, unlike analogous Pd(II) complexes with either α-diimines[18b] or pyridylimines[25] or pyridylidene amides,[26] in this case moving from neutral to cationic and, for the latter, from acetonitrile to lutidine derivatives, no variation in the chemical shift of the Pd–CH_3 peak was observed, thus suggesting that the variation in the electronic density on the metal center is modulated by the phosphorus donor ligand.

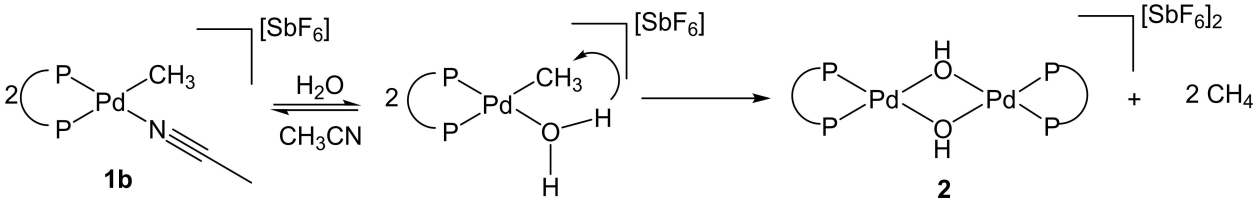

Scheme 2. Proposed mechanism for the formation of **2**.

Reactivity of 1 b with ethylene

The reactivity of complex **1 b** with ethylene was studied by *in situ* NMR spectroscopy, by bubbling the gaseous monomer into a 10 mM solution of [Pd(**1**)(CH_3)($NCCH_3$)][SbF_6] in CD_2Cl_2 at room temperature. An instant change in the color of the solution was observed during bubbling, from pale yellow to light red (Figure 5).

In the ^{1}H-NMR spectrum recorded 10 minutes after the saturation with ethylene no signal of **1 b** is present, whereas the peaks of free acetonitrile, **2** and several other resonances in the aliphatic and vinylic region are observed. The formation of **2** is due to the presence of traces of water both in the deuterated solvent and in ethylene. After 30 minutes, no variation in intensity for the peak of **2** is evident, indicating that, under the applied reaction conditions, not only **2** is inert towards ethylene, but also its formation is inhibited (Figure 6).

Some of the signals in the aliphatic and vinylic region of the ^{1}H-NMR spectrum were easily assigned, according to literature,[19,27] to *cis*-2-butene (1.60 ppm), *trans*-2-butene (1.62 ppm) with the *cis* isomer prevailing, propene (1.71 ppm) and ethane (0.85 ppm) (Figure 7, Figures S23, S24). The intensity of these and other peaks (see below) increases with time (Figures S23, S24), with *cis*-2-butene preferentially formed (*cis*/*trans* = 85/15 at t = 30 min).

On the basis of bidimensional multinuclear NMR experiments (Figures S25–S27) it was possible to assign all the other signals. According to the ^{1}H,^{13}C-HSQC experiment (Figure S26), the triplets between 0.88 and 1.07 ppm are assigned to methyl groups, and the multiplets in the range 1.25–1.52 ppm as well as those ones between 1.98–2.10 ppm are attributed to the relevant methylenic protons. These resonances are due to 1-butene (0.97 and 2.05 ppm), 2- and 3-hexene (0.88, 1.35, 2.00 ppm and 0.93 and 2.03 ppm, respectively). The multiplets centered at 1.03 and 1.48 ppm are due to the Pd–CH_2CH_3 fragment of a palladium intermediate containing the diphosphine, as indicated by the correlation peaks observed in the ^{1}H,^{31}P-HMBC spectrum (Figure S27). The CH_2^{α} resonances of the ligand skeleton in the Pd-compounds present in solution are also assigned on the basis of the ^{1}H,^{31}P-HMBC spectrum (Figure S27): the singlet at 3.49 ppm is due to the Pd–CH_2CH_3 intermediate, the signal at 3.54 ppm to **2**, and those at 3.57 and 3.58 ppm to other Pd-species. Indeed, in the ^{31}P-NMR spectrum in addition to the two doublets at 28.7 and −0.5 ppm due to the Pd-ethyl species, and to the singlet of **2**, there are two multiplets, centered at −2.6 and 21.4 ppm, respectively, together with a peak of low intensity at 46.9 ppm (Figure S28b), due to a Pd-compound already present in traces in **1 b**. With the aim to gain more information about these species, the solvent was removed from the light red solution leading to palladium metal and a light red solid that was analyzed by NMR spectroscopy, ESI-MS spectrometry in solution, and X-ray diffractometry in solid state.

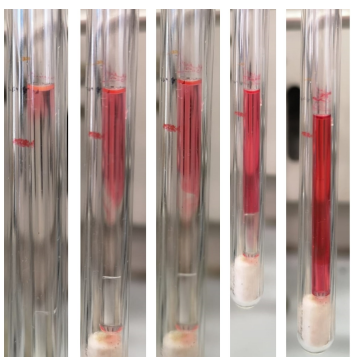

Figure 5. Color changes of the [Pd(**1**)(CH_3)($NCCH_3$)][SbF_6] **1 b** CD_2Cl_2 solution during ethylene bubbling.

Single crystals suitable for X-ray analysis were obtained upon layering n-hexane on the CD_2Cl_2 solution used for the NMR characterization of the light red solid kept at 277 K for three days. Several crystals were used to collect the diffraction figures, leading to two data sets.

X-ray analysis showed that the batch obtained with the double layer technique contained two different types of crystals, visually indistinguishable at the microscope. The structure of the first type of crystals, referred to as S_{anti} in the following, could be solved and refined satisfactorily to a final R value of 3.87 % (Table S1); on the other hand, and probably due to poor quality of the diffraction images, the structure of the second type of crystals, which we will quote as S_{syn} in the following, could only be solved, but refinement was unsatisfactory. The primitive cell of the S_{anti} structure contains a single molecule of a dinuclear palladium species of formula [Pd(μ-η^2–C_6H_5)PPh)–PPh_2]$_2$[SbF_6]$_2$, **3**, (only "half" molecule is crystallographically independent) (Figure 8). Each Pd atom of the dimer is bonded to the two P atoms of ligand **1**, the planar four-fold coordination being completed by a Pd–Pd interaction (2.6971(5) Å) and an η^2 bond with one of the π orbitals of a phosphine phenyl ring (each Pd atom interacts with the phenyl group of the ligand on the other Pd, see Figure 8; Pd–C bond

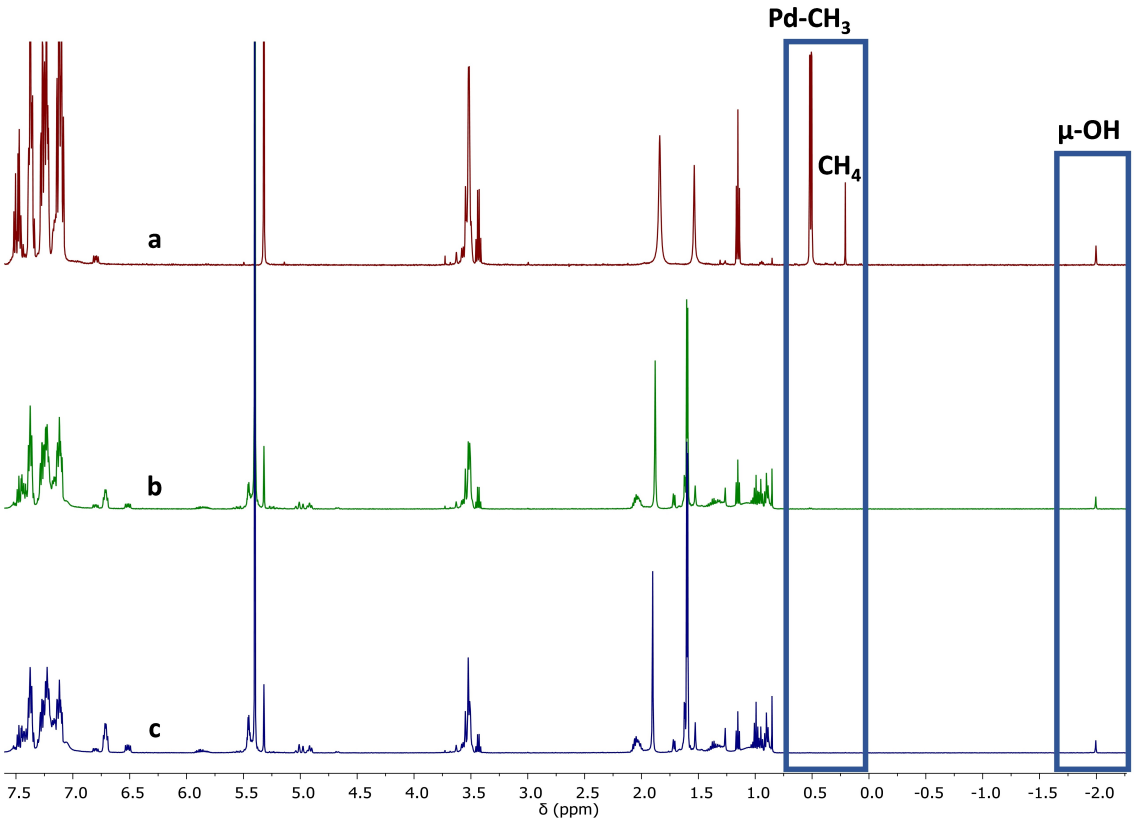

Figure 6. ^{1}H-NMR spectra in CD_2Cl_2 at 298 K of: a) **1 b**; b) **1 b** + ethylene at: t = 10 min; c) t = 30 min.

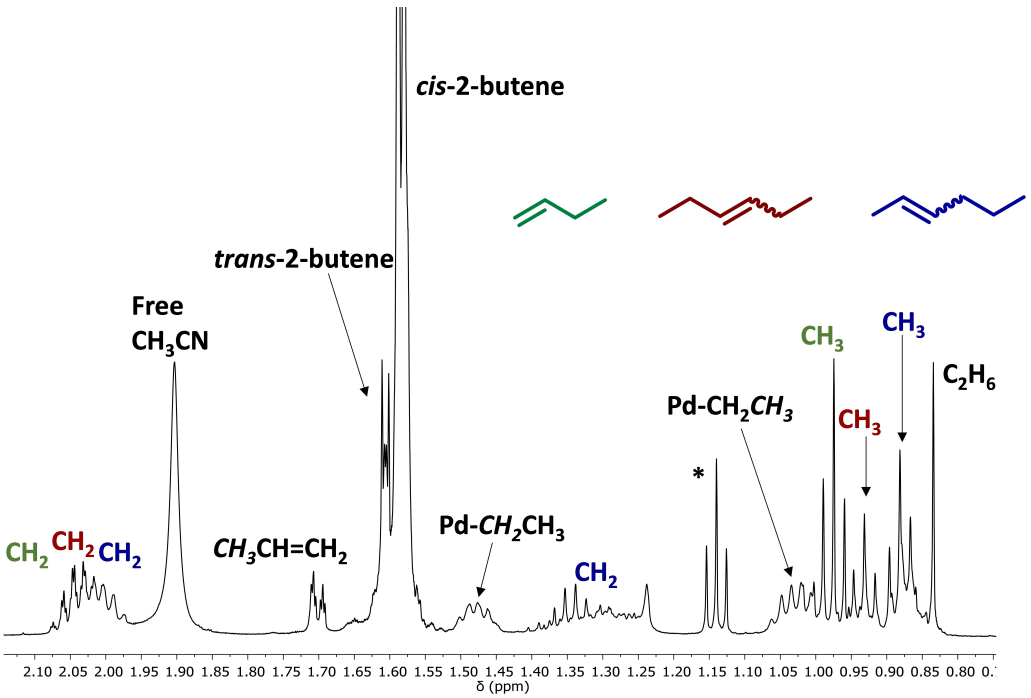

Figure 7. ^{1}H-NMR spectrum (CD_2Cl_2, 273 K) of **1 b** + ethylene, at t = 30 min, aliphatic region (* = diethyl ether).

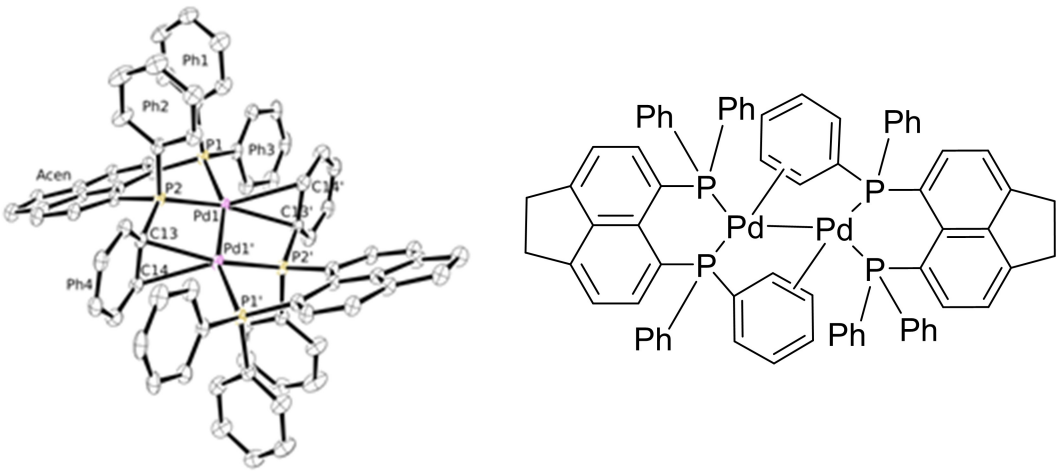

Figure 8. ORTEP representation of complex **3** (left) and its drawing (right). Selected bond distances (Å) and angles (°): Pd1–C13′ 2.357(2), Pd1–C14′ 2.543(2), Pd1–P1 2.3299(7), Pd1–P2 2.2109(6), Pd1–Pd1′ 2.6971(5); C13′–Pd1–C14′ 33.22(7)°, C13′–Pd1–Pd1′ 86.69(5), C14′–Pd1–Pd1′ 98.71(5)°, P2–Pd1–P1 90.00(2)°, P2–Pd1–Pd1′ 68.99(2)°, Pd1–Pd1′–P2 47.30(2), dihedral angles [Acen]–[Pd1] 46.52(3)°, [Ph1]–[Pd1] 86.35(6)°, [Ph2]–[Pd1] 59.30(7)°, [Ph3]–[Pd1] 59.30(7)°, [Ph4]–[Pd1] 67.55(6)°.

lengths: 2.357(2) Å and 2.543(2) Å). The Pd–Pd distance is in line with values found in similar Pd(I) dimeric complexes.[28] Pd(I)-phenyl η^2 coordination is not uncommon.[29]

The average plane of the acenaphthene group of ligand **1** is not coplanar with the corresponding Pd equatorial plane, making a dihedral angle of 46.52(3)° with the latter. The coordination planes of the two Pd ions (which are symmetry mates in the unit cell) are coplanar. The phenyl groups on each phosphine moiety are oriented such that two of them (one per each P atom) are orthogonal with respect to the Pd coordination plane (dihedral angles: 86.35(6)° and 83.27(7)°) and parallel to each other, giving rise to a π-π interaction (see Ph1 and Ph2 in Figure 8). The bending of the acenaphthene groups establishes the possibility of a *syn*/*anti* configuration, where the acenaphthene moieties are bent towards the same (*syn*) or opposite (*anti*) side with respect to the Pd coordination plane. In structure S_{anti} the configuration of the acenaphthene groups is of *anti* type and the same holds for the orientation of the Ph1 and Ph2 groups (Figure 8, Figure S31). As already said, we were unable to refine structure S_{syn}. Nevertheless, the raw solution unequivocally showed that the S_{syn} crystals are actually co-crystals where the unit cell contains a molecule of complex **3** packed with a molecule of the μ-hydroxo complex **2**, which we already structurally characterized (Figure 4). Even if we cannot quote precise distances and angles in the S_{syn} structure, from its solution it is evident that in this latter the configuration of the acenaphthene and Ph1 and Ph2 groups is of *syn* type. The different geometries of complex **3** in the S_{anti} and S_{syn} structures are compared in Figure S31.

The structure in solid state agrees with the NMR characterization in solution. Indeed, the signals observed in both ^{1}H and ^{31}P-NMR spectra of the CD_2Cl_2 solution of the light red solid indicate that this solid is a mixture of **2** and **3**, plus traces of the unknown species (Figures S28c, S29). In the ^{31}P-NMR spectrum the two multiplets at −2.6 and 21.4 ppm are reasonably due to the overlap of the phosphorus signals in the S_{anti} and S_{syn} configurations of the acenaphthene moieties in the two dimers found in solid state.

The ESI-MS spectrum confirms the nature of **3** (Figure S32).

A CD_2Cl_2 solution of the light red solid was saturated with ethylene at room temperature, but no reaction was observed within 2 h, indicating that, under these conditions, **3**, in analogy with **2**, is an inert compound.

On the basis of the studies reported above, it is possible to state that **1b** is a catalyst for the ethylene dimerization and trimerization, leading to the preferential formation of *cis*-2-butene, and to propose a mechanism for the catalytic reaction.

The presence of propene indicates that, in agreement with literature,[26–27,30] the activation of **1b** takes place via the substitution of acetonitrile with ethylene, followed by its migratory insertion reaction into the Pd–CH_3 bond, and a subsequent β–H elimination (Scheme 3), thus obtaining propylene and the Pd-hydride **ii** as catalytically active species. Here the coordination-insertion of another ethylene molecule takes place, leading to the species having the Pd–CH_2CH_3 fragment **iv**, which represents the catalyst resting state. The latter might follow different pathways involving either the reaction with other ethylene molecules, or its decomposition with the formation of **3** and ethane through either the attack of proton from adventitious water or the homolytic cleavage of the Pd–C bond. In the case of further reactivity with ethylene, the undetected Pd-n-butyl intermediate **v** should form, which can insert another ethylene molecule leading to the Pd-(n-hexyl) species **vi** which rapidly isomerizes with formation of 2- and 3-hexenes and the Pd–H **ii**. As an alternative pathway, **v** might undergo β–H elimination to **vii** which in turn might either dissociate 1-butene with formation of the Pd–H species, or reinsert with opposite regiochemistry leading to the branched intermediate **viii**. On the latter β–H elimination occurs with the preferential formation of *cis*-2-butene. The selectivity

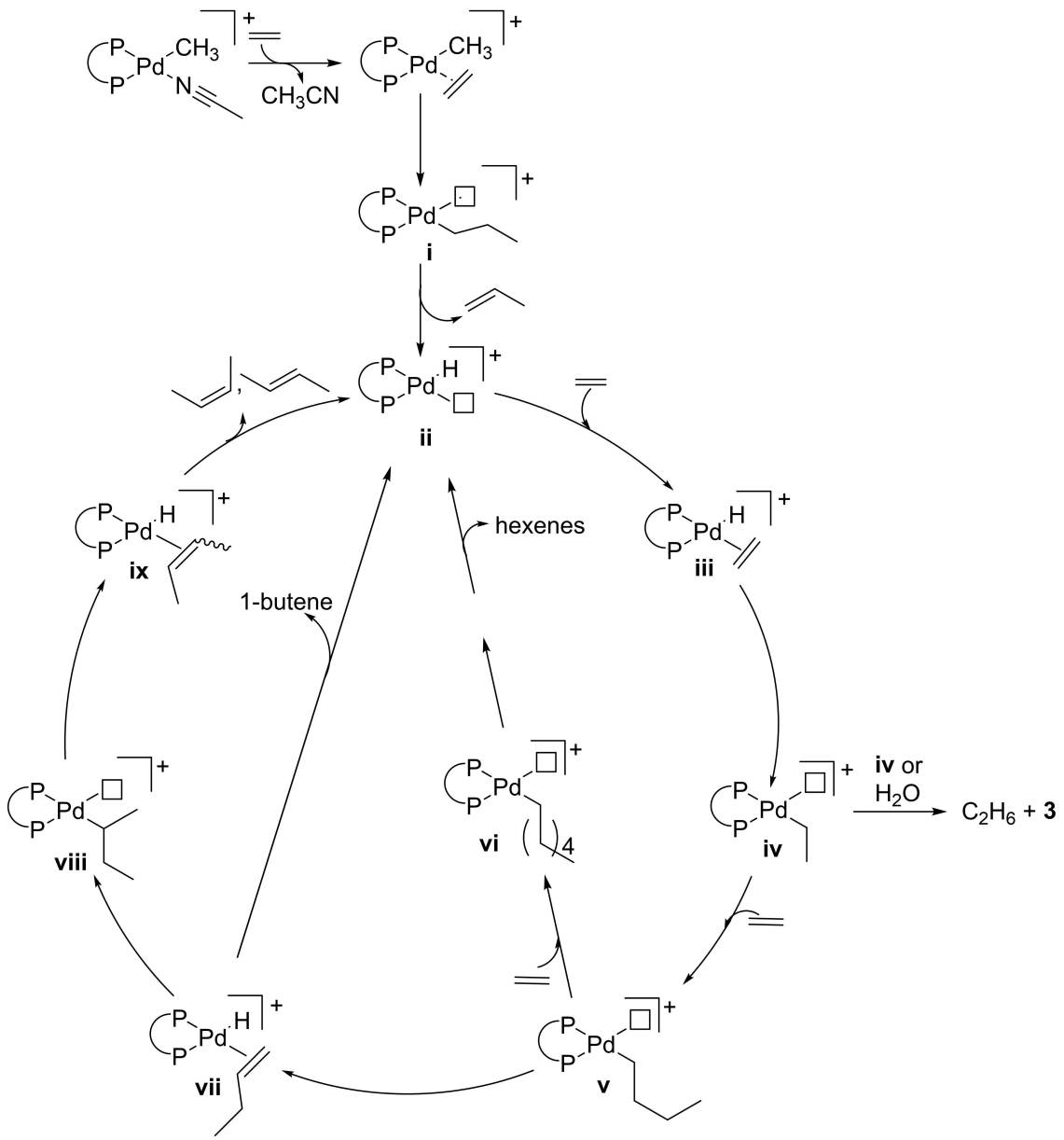

Scheme 3. Proposed catalytic cycle for alkene synthesis catalyzed by **1 b**.

towards the *cis* isomer might be due to the steric hindrance created on palladium by the phenyl rings of the diphosphine ligand, which favors the formation of the 4-membered transition state for the β–H elimination locating both methyl groups on the organic fragment far away from palladium.

This study suggests that for the palladium complex under investigation both migratory insertion reaction of the alkene into the Pd-alkyl bond and the following β–H elimination are remarkably slowed down. This result is in agreement with reported DFT calculations,[31] where the energy barriers for subsequent ethylene migratory insertion reactions were computed for both Pd-diphosphine and Pd-phosphinobenzene sulfonate derivatives. The comparison points out that the migratory insertion reaction of ethylene into the Pd-alkyl bond for the P–P derivative is 7.0 kcal/mol higher than for the P–O one.

With the aim to favor ethylene insertion over β–H elimination, a few catalytic experiments of ethylene homopolymerization were performed at an ethylene pressure of either 20 or 40 bar by using both **1 a** and **1 b** as precatalysts. The catalytic reactions were carried out in dichloromethane as solvent at either 298 or 323 K (Table S2). In addition, in the case of **1 a**, $NaSbF_6$ was added *in situ* as chloride abstracting agent. The catalytic products were isolated as oils.

Both complexes generated very low productive catalysts (productivity values are in the range 18.8–28.2 grams of products per gram of palladium) and for **1 a** a slight increase in

productivity was found on increasing the reaction temperature, whereas no effect was observed on doubling ethylene pressure.

The products are low molecular weight polyethylene (M_n values are in the range 2.1–2.7 kDa) made of branched macromolecules. It should be noted that a remarkable decrease in the branching degree was found moving from the cationic to the neutral catalyst. In addition, the obtained polyethylene has an M_n value four times as high as that of the oligomers produced with the Brookhart's Pd-(**L18**) catalyst.[16]

Conclusions

In this work, the coordination chemistry of the P–P ligand **1** to palladium(II) has been explored, synthesizing the neutral complex [Pd(**1**)(CH_3)Cl] **1 a** and the cationic complexes **1 b–c** [Pd(**1**)(CH_3)(L)][SbF_6] (**1b**, L = CH_3CN; **1 c**, L = 3,5-lutidine). All the complexes have been characterized in solution with mono- and bidimensional NMR spectroscopy. Complex **1b** is sensitive to traces of water in the solvents, which cause its conversion to the dimeric species **2**, [Pd(μ-OH)(**1**)]$_2$[SbF_6]$_2$, characterized by means of both NMR and X-ray diffraction. This kind of reactivity of **1b** was quenched by substitution of the labile ligand CH_3CN with the more strongly coordinating 3,5-lutidine.

The reactivity of **1 b** towards ethylene has been studied by *in situ* NMR spectroscopy. The reaction with ethylene competes with that of water, but the latter is inhibited by ethylene itself; moreover, complex **2** is inert toward ethylene. **1 b** resulted to be an efficient catalyst for the synthesis of butenes and internal hexenes, with a preferential selectivity towards *cis*-2-butene. Propene and ethane were also detected. All the products were recognized and analyzed through 1D and 2D NMR spectroscopy. Among the several organometallic species that can be formed during the reaction, the Pd–CH_2CH_3 intermediate represents the resting state of the catalyst. During the reaction of **1 b** with ethylene, the color of the solution changed from light yellow to light red. This variation was attributed to the formation of the dimeric species **3** [Pd(μ-η^2–C_6H_5)PPh)–PPh_2]$_2$[SbF_6]$_2$, where each Pd ion is η^2-bonded to one of the phenyl groups of the ligand on the other Pd.

The formation of the dimeric complex has been confirmed by NMR spectroscopy, ESI-MS and X-ray diffraction.

The presence of all the organic and organometallic products originated by the reaction of **1 b** with ethylene allows to propose a reaction mechanism, in which the two processes typically involved in the polymerization of olefins, i.e. the migratory insertion of ethylene into the Pd-ethyl bond and beta-hydride elimination, are slowed down.

Homopolymerization tests using ethylene at high pressure have been performed with both **1 a** and **1 b**, and the catalytic products isolated as oils. The two palladium complexes generate catalysts with low activity, and produce branched, low MW polyethylene.

Despite the scarce performances in polymerization, the results obtained from the reactivity experiments concerning the production of butenes and hexenes represent a promising starting point for further development of the system. Moreover, they also point out that Pd-catalysts based on P–P ligands are more delicate than those based on N–N molecules, being more sensitive to traces of water into the reaction mixture.

Experimental Section

All complex manipulations were performed using standard Schlenk techniques under argon. Deuterated solvents (Cambridge Isotope Laboratories, Inc. (CIL)) were stored as recommended by CIL. Palladium(II) neutral complexes were synthesized using [Pd(cod)(CH_3)Cl], synthesized from [Pd($OCOCH_3$)$_2$] (BASF Italia), benzonitrile (Sigma-Aldrich), HCl 37% (Fluka) and cis-cis-1,5-cyclooctadiene (Fluka) without further purification. The cationic complexes were synthesized by using $AgSbF_6$ and anhydrous acetonitrile (Sigma-Aldrich). Dichloromethane (Sigma-Aldrich) used in the synthesis of Pd complexes was distilled over CaH_2 under argon atmosphere. Ethylene was purchased from SIAD and used as such for reactivity NMR experiments. Mono- and bidimensional NMR spectra were recorded on a Varian 500 spectrometer (500 MHz for ^{1}H, 125.68 MHz for ^{13}C, 202.4 MHz for ^{31}P), or on a Varian 400 (400 MHz for ^{1}H, 100.55 MHz for ^{13}C, 161.9 MHz for ^{31}P), using the residual solvent peak as reference (CD_2Cl_2: 5.32 ppm for ^{1}H-NMR, 54.00 ppm for ^{13}C-NMR; $CDCl_3$: 7.26 ppm for ^{1}H-NMR, 77.16 ppm for ^{13}C-NMR). Mass spectra (ESI-MS) were recorded on a Massa Esquire 4000–Bruker in positive ion polarity (HV capillary of 4000 V and dry gas of 5.00 L/min). The analysis was carried out immediately after samples were dissolved in methanol.

Synthesis and characterization of ligand 1

Ligand **1** was synthesized according to the literature procedure.[17]

1. (pale yellow solid, 90%) ^{1}H-NMR (400 MHz, $CDCl_3$, 298 K) δ 7.28–7.23 (m, 24H), 3.43 (s, 4H); ^{1}H-NMR (400 MHz, CD_2Cl_2) δ = 7.30–7.21 (m, 16H), 7.20–7.15 (m, 8H), 3.41 (s, 4H); ^{13}C-NMR (101 MHz, CD_2Cl_2) δ = 149.2, 139.9, 139.8, 139.7, 138.6, 138.5, 138.2, 138.0, 133.8, 133.7, 133.6, 130.5, 130.4, 130.2, 128.3, 128.2, 128.1, 127.9, 119.9, 30.0; ^{31}P-NMR (162 MHz, $CDCl_3$) δ = −17.7; ^{31}P-NMR (162 MHz, CD_2Cl_2) δ = −16.2. IR: (KBr disc, cm^{-1}) $\tilde{\nu}$ = 3069 m, 3049 m, 2927 m, 1603 m, 1568 m, 1478 m, 1434 s, 1326 m, 1263w, 1186w, 1113w, 1089w, 1064w, 1028w, 844w, 744 s, 699 s. ESI-MS (m/z): 561.2 $[M+K]^+$.

Synthesis and characterization of the neutral complex [Pd(1)(CH_3)Cl], 1 a. To 1 equiv. of [Pd(cod)(CH_3)Cl] dissolved in 10 mL of distilled dichloromethane, 1.2 equiv. of ligand **1** were added. The solution was left under stirring at room temperature (2 h). The solution was further concentrated under reduced pressure and diethyl ether was added to favor the complete precipitation of the product. The yellow precipitate was then filtered and washed with additional cold diethyl ether, then dried under vacuum.

1 a. (beige solid, 87%) ^{1}H-NMR (500 MHz, CD_2Cl_2, 298 K) δ = 7.41–7.36 (m, 2H, H^{γ}), 7.34–7.24 (m, 10H, $Ph^{Hm/o}$, H^{β}), 7.22–7.16 (m, 12H, $Ph^{Hp,Hm/o}$), 3.46 (s, 4H, CH_2^{α}), 0.51 (dd, J = 8.1, 3.2 Hz, 3H, Pd–CH_3); ^{13}C-NMR (101 MHz, CD_2Cl_2) δ = 140.6, 140.1 (C^{γ}), 134.1, 130.9, 129.8, 128.5 (Ar–C), 120.7, 120.1 (C^{β}), 30.6 (CH_2^{α}), 15.6 (Pd–CH_3); ^{31}P-NMR (202 MHz, CD_2Cl_2, 298 K) δ = 30.0 (d, J = 65.5 Hz), 1.4 (d, J = 65.5 Hz). Elemental analysis for $C_{37}H_{31}P_2PdCl$ (%): theoretical: C = 65.39%, H = 4.60%; Experimental: C = 65.85%, H = 4.77%.

Synthesis and characterization of the cationic complexes [Pd(1)(CH_3)(L)][SbF_6] (L = CH_3CN, lut), 1 b–1 c. To 1 equiv. of the neutral precursor **1 a** dissolved in 6 mL of distilled dichloromethane, 1.2 equiv. of $AgSbF_6$ salt dissolved in 1.5 mL of dry acetonitrile were added. The reaction mixture was left under stirring in the dark for 45 min. The suspension of AgCl was filtered over Celite® and

washed with dichloromethane. The solution was then concentrated under reduced pressure and diethyl ether was added to induce the precipitation of the product. The bright yellow solids were then filtered under reduced pressure, washed with cold diethyl ether and dried under vacuum.

1 b. (yellow solid, 47 %) ^{1}H-NMR (500 MHz, CD_2Cl_2, 298 K) δ = 7.52–7.45 (m, 2H, H^{β}, H^{γ}), 7.41–7.37 (m, 6H, Ph^{Hp}, H^{β}, H^{γ}), 7.32–7.22 (m, 8H, Ph^{Hm}), 7.21–7.10 (m, 8H, Ph^{Ho}), 3.55–3.48 (m, 4H, CH_2^{α}), 1.84 (s, 3H, Pd-NCCH$_3$), 0.51 (dd, J = 5.3, 2.3 Hz, 3H, Pd–CH$_3$); ^{13}C-NMR (101 MHz, CD_2Cl_2) δ = 140.7, 140.0 (C^{γ}), 139.5, 133.3, 132.6, 130.9, 128.7 ($Ph^{Hp,Ho,Hm}$), 120.9, 120.2 (C^{β}), 30.6 (CH_2^{α}), 15.6 (Pd–CH$_3$); ^{31}P-NMR (202 MHz, CD_2Cl_2, 298 K) δ = 29.8 (d, J = 67.2 Hz), 20.1 (s), −0.1 (d, J = 67.1 Hz). Elemental analysis for $C_{39}H_{34}P_2SbPdNF_6$: theoretical: C = 50.86 %, H = 3.73 %, N = 1.52 %. experimental: C = 50.40 %, H = 4.04 %, N = 1.60 %.

1 c. (orange solid, 54 %) ^{1}H-NMR (500 MHz, CD_2Cl_2, 298 K) δ = 7.89 (s, 2H, $^{Lut}H^{2,6}$), 7.58–7.55 (dd, J = 10.6, 7.3 Hz, 1H, H^{γ}), 7.48–7.40 (m, 3H, H^{β}, Ph^{Hp}), 7.38–7.33 (m, 6H, H^{β}, H^{γ}, Ph^{Hp}), 7.33–7.27 (m, 4H, Ph^{Hm}), 7.26–7.18 (m, 7H, $Ph^{Hp,o}$, $^{Lut}H^{4}$), 7.07 (td, J = 7.9, 2.3 Hz, 4H, Ph^{Hm}), 6.95 (ddt, J = 11.1, 7.4, 1.3 Hz, 4H, Ph^{Ho}), 3.56–3.48 (m, 4H, CH_2^{α}), 2.09 (s, 6H, $^{Lut}CH_3$), 0.48 (dd, J = 7.2, 2.7 Hz, 3H, Pd–CH$_3$). ^{13}C-NMR (125.68 MHz, CD_2Cl_2, 298 K) δ = 148.4 ($^{Lut}C^{2,6}$), 141.5, 139.5 (C^{γ}), 139.4 ($^{Lut}C^{4}$), 133,6, 133.4 (C Ph^{Ho}), 131.6, 130.9 (C Ph^{Hp}), 128.9 (C Ph^{Hm}), 121.1, 120.8 (C^{β}), 30.9 (CH_2^{α}), 18.4 ($^{Lut}CH_3$), 17.4 (Pd–CH$_3$). ^{31}P-NMR (162 MHz, CD_2Cl_2, 298 K) δ = 28.8 (d, J = 61.9 Hz), 1.8 (d, J = 62.3 Hz). Elemental analysis for $C_{44}H_{40}P_2SbPdNF_6$: theoretical: C = 53.54 %, H = 4.09 %, N = 1.42 %; experimental: C = 54.00 %, H = 4.29 %, N = 1.49 %.

Synthesis and characterization of the cationic complex [Pd(1)(μ-OH)]$_2$[SbF$_6$]$_2$, 2. Synthesis of **2** was performed at room temperature and ambient atmosphere. In 6 mL of non-anhydrous dichloromethane 0.0389 mmol of **1 b** were dissolved. The solution was left under stirring for 24 h, keeping the volume of the solution constant. The solution was then concentrated at reduced pressure and diethyl ether was added to precipitate the product. The obtained white solid was filtered under reduced pressure and washed with additional diethyl ether.

2. (white solid, 52 %) ^{1}H-NMR (500 MHz, CD_2Cl_2, 298 K) δ = 7.48 (d, J = 7.4 Hz, 4H, H^{γ}), 7.37 (t, J = 7.4 Hz, 8H, Ph^{Hp}), 7.26–7.20 (m, 20H, H^{β}, Ph^{Hm}), 7.16 (ddd, J = 12.8, 8.0, 1.4 Hz, 16H, Ph^{Ho}), 3.54 (s, 8H, CH_2^{α}), −2.00 (s, 2H, μ-OH). ^{13}C-NMR (125.68 MHz, CD_2Cl_2, 298 K) δ = 139.4 (C^{γ}), 133.3, 132.7, 129.1 (Ar–C), 121.1 (C^{β}), 30.8 (CH_2^{α}). ^{31}P-NMR (202 MHz, CD_2Cl_2, 298 K) δ = 20.1 (s). Elemental analysis for $C_{72}H_{58}P_4Sb_2Pd_2O_2F_{12}$: theoretical: C = 53.74 %, H = 3.64 %; experimental: C = 54.05 %, H = 3.60 %.

Ethylene homopolymerization. Ethylene polymerizations were carried out in a stainless steel autoclave equipped with a magnetic stirrer. The reactor was first dried overnight at 120 °C in an oven, cooled under vacuum, then preconditioned with ethylene by means of three pressure/vent cycles. The reactor was thermostated at defined temperatures, charged with 20 ml of dichloromethane, the catalyst and $NaSbF_6$ as counter ion and then pressurized at the prescribed ethylene pressure. The mixture was stirred for the programmed time under constant ethylene pressure. Before quenching the polymerization reaction, a small amount of solution was taken for GC analysis. The resulting solution was treated with hexane and water, then the organic layer was dried over $MgSO_4$, filtered and the volatiles were distilled off in a rotavapor. The resulting oily residue was dried under vacuum overnight at 80 °C.

In situ NMR reactivity of complex 1 b with ethylene. Ethylene was bubbled for 10 minutes in a 10 mM solution in CD_2Cl_2 of complex **1 b**. The reaction was monitored over time with mono- and bidimensional NMR experiments, both at 298 K and 273 K, to follow the disappearance of Pd–CH$_3$ signal of **1 b** and to characterize the new formed species.

X-ray crystallography. Data collections for crystals of **2** and **3** were performed at the X-ray diffraction beamline (XRD1) of the Elettra Synchrotron of Trieste (Italy) equipped with a Pilatus 2 M image plate detector. Collection temperature was 100 K (nitrogen stream supplied through an Oxford Cryostream 700); the wavelength of the monochromatic X-ray beam was 0.700 Ångström and the diffractograms were obtained with the rotating crystal method. The crystals were dipped in N-paratone and mounted on the goniometer head with a nylon loop. The diffraction data were indexed, integrated and scaled using the XDS code.[32] The structures were solved by the dual space algorithm implemented in the SHELXT code.[33] Fourier analysis and refinement were performed by the full-matrix least-squares methods based on F^2 implemented in SHELXL.[34] The Shelxle program was used for modeling.[35] Anisotropic thermal motion was allowed for all non- hydrogen atoms. Hydrogen atoms were placed at calculated positions with isotropic factors U = 1.2 × Ueq, where Ueq is the equivalent isotropic thermal factor of the bonded non hydrogen atom.

Crystal data and details of refinements are given in Table S1.

Deposition Numbers 2191647 (**2**) and 2191646 (**3**) contain the supplementary crystallographic data for this paper. These data are provided free of charge by the joint Cambridge Crystallographic Data Centre and Fachinformationszentrum Karlsruhe Access Structures service www.ccdc.cam.ac.uk/structures.

Supporting Information (See footnote on the first page of this article): NMR characterization of ligand and complexes, X-ray characterization, NMR in situ studies, catalytic data (pdf).

Acknowledgments

This work was financially supported by Università degli Studi di Trieste (B. M. and C. A. FRA 2022). Fondazione Beneficentia Stiftung is gratefully acknowledged for cofinancing the fellowship to A. DA. The Ph.D. fellowship of C. A. was supported by FSE-PO2014/2020 and Regione FVG, Program 89/19.

Conflict of Interest

The authors declare no conflict of interest.

Data Availability Statement

The data that support the findings of this study are available in the supplementary material of this article.

Keywords: Ethylene oligomerization · Homogeneous catalysis · P ligands · Palladium · Reaction mechanisms

[1] S. D. Ittel, L. K. Johnson, M. Brookhart, *Chem. Rev.* **2000**, *100*, 1169–1204.
[2] A. Nakamura, T. M. J. Anselment, J. Claverie, B. Goodall, R. F. Jordan, S. Mecking, B. Rieger, A. Sen, P. Van Leeuwen, K. Nozaki, *Acc. Chem. Res.* **2013**, *46*, 1438–1449.
[3] a) S. L. J. Luckham, K. Nozaki, *Acc. Chem. Res.* **2021**, *54*, 344–355; b) R. S. Birajdar, S. H. Chikkali, *Eur. Polym. J.* **2021**, *143*, 110183; c) F. Wang, C.

Chen, *Polym. Chem.* **2019**, *10*, 2354–2369; d) Z. Chen, M. Brookhart, *Acc. Chem. Res.* **2018**, *51*, 1831–1839; e) B. P. Carrow, K. Nozaki, *Macromolecules* **2014**, *47*, 2541–2555; f) N. M. G. Franssen, J. N. H. Reek, B. de Bruin, *Chem. Soc. Rev.* **2013**, *42*, 5809–5832; g) F. Wang, R. Tanaka, Q. Li, Y. Nakayama, J. Yuan, T. Shiono, *J. Mol. Catal. A* **2015**, *398*, 231–240.

[4] Y. Mitsushige, B. P. Carrow, S. Ito, K. Nozaki, *Chem. Sci.* **2016**, *7*, 737–744.

[5] a) X. Sui, S. Dai, C. Chen, *ACS Catal.* **2015**, *5*, 5932–5937; b) W. Zhang, P. M. Waddell, M. A. Tiedemann, C. E. Padilla, J. Mei, L. Chen, B. P. Carrow, *J. Am. Chem. Soc.* **2018**, *140*, 8841–8850.

[6] a) R. Nakano, K. Nozaki, *J. Am. Chem. Soc.* **2015**, *137*, 10934–10937; b) W. Tao, S. Akita, R. Nakano, S. Ito, Y. Hoshimoto, S. Ogoshi, K. Nozaki, *Chem. Commun.* **2017**, *53*, 2630–2633.

[7] E. Drent, P. H. M. Budzelaar, *Chem. Rev.* **1996**, *96*, 663–681.

[8] D. Peng, W. Pang, G. Xu, C. Tan, F. Wang, *Appl. Organomet. Chem.* **2019**, *33*, e5054.

[9] Q. Wu, W. Wang, G. Xu, W. Pang, Y. Li, C. Tan, F. Wang, *Appl. Organomet. Chem.* **2020**, *34*, e5428.

[10] a) I. Albers, E. Álvarez, J. Cámpora, C. M. Maya, P. Palma, L. J. Sánchez, E. Passaglia, *J. Organomet. Chem.* **2004**, *689*, 833–839; b) N. A. Cooley, S. M. Green, D. F. Wass, K. Heslop, A. G. Orpen, P. G. Pringle, *Organometallics* **2001**, *20*, 4769–4771; c) J. N. L. Dennett, A. L. Gillon, K. Heslop, D. J. Hyett, J. S. Fleming, C. E. Lloyd-Jones, A. G. Orpen, P. G. Pringle, D. F. Wass, J. N. Scutt, R. H. Weatherhead, *Organometallics* **2004**, *23*, 6077–6079; d) M. Schultz, F. Eisenträger, C. Regius, F. Rominger, P. Hanno-Igels, P. Jakob, I. Gruber, P. Hofmann, *Organometallics* **2012**, *31*, 207–224.

[11] A. L. Kocen, M. Brookhart, O. Daugulis, *Nat. Commun.* **2019**, *10*, 438.

[12] D. Bézier, O. Daugulis, M. Brookhart, *Organometallics* **2017**, *36*, 2947–2951.

[13] a) Y. Zhang, Y. Cao, X. Leng, C. Chen, Z. Huang, *Organometallics* **2014**, *33*, 3738–3745; b) N. R. Mote, S. R. Gaikwad, K. V. Khopade, R. G. Gonnade, S. H. Chikkali, *Dalton Trans.* **2021**, *50*, 3717–3723.

[14] N. D. Contrella, R. F. Jordan, *Organometallics* **2014**, *33*, 7199–7208.

[15] Z. Cai, Z. Shen, X. Zhou, R. F. Jordan, *ACS Catal.* **2012**, *2*, 1187–1195.

[16] D. Bézier, O. Daugulis, M. Brookhart, *Organometallics* **2017**, *36*, 443–447.

[17] M. Tosolini, J. Avó, A. J. Parola, G. Balducci, P. Tecilla, *Eur. J. Inorg. Chem.* **2020**, *2020*, 3859–3868.

[18] a) L. K. Johnson, S. Mecking, M. Brookhart, *J. Am. Chem. Soc.* **1996**, *118*, 267–268; b) A. Meduri, T. Montini, F. Ragaini, P. Fornasiero, E. Zangrando, B. Milani, *ChemCatChem* **2013**, *5*, 1170–1183.

[19] V. Khlebnikov, A. Meduri, H. Mueller-Bunz, T. Montini, P. Fornasiero, E. Zangrando, B. Milani, M. Albrecht, *Organometallics* **2012**, *31*, 976–986.

[20] A. Dall'Anese, V. Rosar, L. Cusin, T. Montini, G. Balducci, I. D'Auria, C. Pellecchia, P. Fornasiero, F. Felluga, B. Milani, *Organometallics* **2019**, *38*, 3498–3511.

[21] J. Durand, E. Zangrando, M. Stener, G. Fronzoni, C. Carfagna, B. Binotti, P. C. J. Kamer, C. Muller, M. Caporali, P. W. N. M. van Leeuwen, D. Vogt, B. Milani, *Chem. Eur. J.* **2006**, *12*, 7639–7651.

[22] a) C. Bianchini, A. Meli, G. Müller, W. Oberhauser, E. Passaglia, *Organometallics* **2002**, *21*, 4965–4977; b) C. Bianchini, A. Meli, W. Oberhauser, A. M. Segarra, C. Claver, E. J. G. Suarez, *J. Mol. Catal. A* **2007**, *265*, 292–305.

[23] S. Alvarez, *Dalton Trans.* **2013**, *42*, 8617–8636.

[24] C. Janiak, *J. Chem. Soc. Dalton Trans.* **2000**, 3885–3896.

[25] a) V. Rosar, D. Dedeic, T. Nobile, F. Fini, G. Balducci, E. Alessio, C. Carfagna, B. Milani, *Dalton Trans.* **2016**, *45*, 14609–14619; b) A. Dall'Anese, M. Fiorindo, D. Olivieri, C. Carfagna, G. Balducci, E. Alessio, J. Durand, B. Milani, *Macromolecules* **2020**, *53*, 7783–7794.

[26] M. Navarro, V. Rosar, T. Montini, B. Milani, M. Albrecht, *Organometallics* **2018**, *37*, 3619–3630.

[27] a) B. Milani, A. Marson, A. Scarel, G. Mestroni, J. M. Ernsting, C. J. Elsevier, *Organometallics* **2004**, *23*, 1974–1977; b) G. M. Ó Máille, A. Dall'Anese, P. Grossenbacher, T. Montini, B. Milani, M. Albrecht, *Dalton Trans.* **2021**, *50*, 6133–6145.

[28] a) Y. N. Lim, S. K. Chae, W. Yim, J.-Y. Park, W. Yoon, H. Yun, E. Kim, S. U. Son, H.-Y. Jang, *Appl. Organomet. Chem.* **2019**, *33*, e4761; b) P. H. M. Budzelaar, P. W. N. M. Van Leeuwen, C. F. Roobeek, A. G. Orpen, *Organometallics* **1992**, *11*, 23–25.

[29] M. Catellani, C. Mealli, E. Motti, P. Paoli, E. Perez-Carreño, P. S. Pregosin, *J. Am. Chem. Soc.* **2002**, *124*, 4336–4346.

[30] A. Tognon, V. Rosar, N. Demitri, T. Montini, F. Felluga, B. Milani, *Inorg. Chim. Acta* **2015**, *431*, 206–218.

[31] K. Nozaki, S. Kusumoto, S. Noda, T. Kochi, L. W. Chung, K. Morokuma, *J. Am. Chem. Soc.* **2010**, *132*, 16030–16042.

[32] W. Kabsch, *Acta Crystallogr. Sect. D* **2010**, *66*, 125–132.

[33] G. M. Sheldrick, *Acta Crystallogr. Sect. A* **2015**, *71*, 3–8.

[34] G. M. Sheldrick, *Acta Crystallogr. Sect. A* **2008**, *64*, 112–122.

[35] C. B. Hübschle, G. M. Sheldrick, B. Dittrich, *J. Appl. Crystallogr.* **2011**, *44*, 1281–1284.